Vol. 712: 21–34, 2023
https://doi.org/10.3354/meps14318

MARINE ECOLOGY PROGRESS SERIES
Mar Ecol Prog Ser

Published June 8

Saline groundwater discharge accelerates phytoplankton primary production in a Sanriku ria coastal embayment, Japan

Toshimi Nakajima[1,*], Takahiro Kusunoki[2], Yoshitake Takao[2], Kazumasa Yamada[2], Katsuhide Yokoyama[3], Ryo Sugimoto[2]

[1]Graduate School of Bioscience and Biotechnology, Fukui Prefectural University, Fukui 917-0003, Japan
[2]Faculty of Marine Biosciences and Technology, Fukui Prefectural University, Fukui 917-0003, Japan
[3]Graduate School of Urban Environmental Sciences, Tokyo Metropolitan University, Tokyo 192-0397, Japan

ABSTRACT: Nutrient supply through submarine groundwater discharge into coastal seas can be critical to primary production. However, the influence of recirculated saline groundwater on phytoplankton primary production has not been fully elucidated. Here, we assessed how saline groundwater discharge stimulates phytoplankton primary production in a semi-enclosed embayment (Kesennuma Bay, Japan). We contrasted offshore nutrient supply conditions during summer (stratified condition) and autumn (vertical mixed condition). First, we measured phytoplankton primary productivity in surface seawater using the stable carbon isotope tracer method and identified water sources based on radium isotopes. Then, bioassay incubation experiments were conducted to determine the nutrients limiting phytoplankton primary production and ascertain the effect of saline groundwater discharge. The results showed that nutrients derived from saline groundwater accounted for 19.3 to 38.3, 7.1 to 19.0, and 12.7 to 21.0% of dissolved inorganic nitrogen, phosphorus, and silica concentrations, respectively, in surface seawater. Furthermore, chl *a*-normalized primary productivity was higher in autumn when the relative contribution of saline groundwater in surface seawater increased. The bioassay experiment showed that phytoplankton growth was most stimulated by a combination of nitrogen and phosphorus, but nitrogen addition enhanced phytoplankton growth in most cases, even at low phosphate concentration (≤0.04 µmol l^{-1}) in seawater. Our findings suggest that input of nitrogen-enriched saline groundwater could mitigate the nitrogen limitation of phytoplankton growth, and can be more effective in the vertically mixed season due to the high contribution of offshore phosphorus to surface water. Overall, saline groundwater discharge can stimulate phytoplankton primary production, and should be considered a significant nutrient source for sustaining biological production in coastal seas.

KEY WORDS: Submarine groundwater discharge · Primary production · Phytoplankton · Radium · Bioassay experiment

1. INTRODUCTION

Phytoplankton primary production in the ocean accounts for approximately 50% of the total primary production on the planet (Field et al. 1998) and plays a vital role in global biogeochemical cycles, such as nutrient and carbon cycling (Falkowski et al. 1998). It also plays an essential role in secondary production (Brett et al. 2009) and subsequent trophic networks, including fisheries production (Chassot et al. 2010). Specifically, the coastal sea is one of the most productive regions in the ocean for primary production (Nixon 1988). The high primary production of coastal seas is primarily sustained by allochthonous nutri-

*Corresponding author: t-nakajima@aori.u-tokyo.ac.jp

ents supplied from oceanic offshore waters (Furuya et al. 1993, Kobayashi & Fujiwara 2008), river inputs (Cloern 1991, Ara et al. 2011), and atmospheric deposition (Jickells 1998, Paerl et al. 2002). In recent years, groundwater has been recognized as a ubiquitous pathway of nutrient delivery from land to various coastal ecosystems (Santos et al. 2021).

Nutrient supply via submarine groundwater discharge (SGD) into coastal seas contributes to coastal primary production in both the water column and the benthic environment (Johannes 1980, Lecher & Mackey 2018, Taniguchi et al. 2019). SGD comprises meteoric fresh groundwater discharge (fresh SGD) and recirculated saline groundwater discharge (saline SGD) (Taniguchi et al. 2002). Fresh SGD supplies nutrients from the degradation of organic matter in the soil and aquifer, from the weathering of mineral phases, and from anthropogenic sources such as fertilizer and sewage (Slomp & Van Cappellen 2004). On the other hand, saline SGD supplies nutrients from the mineralization of organic matter in coastal sediments (Santos et al. 2008). As fresh and saline SGD-derived nutrient fluxes into coastal seas vary in space and time (e.g. Tamborski et al. 2017, Nakajima et al. 2018, Diego-Feliu et al. 2022, Cabral et al. 2023), their magnitudes and contributions can provoke differing phytoplankton responses. The differing properties of fresh and saline groundwater can influence phytoplankton community structure (Liefer et al. 2009, Lecher et al. 2017, Liang et al. 2020) and productivity (Sugimoto et al. 2017). Since there is little study combining field and bioassay assessments on the productivity and growth rate of phytoplankton, the influence of SGD on the productivity and growth rate of phytoplankton remains unclear.

The Sanriku ria coast is characterized by small embayments formed from numerous flooded valleys. Coastal currents such as the Tsugaru Warm, Oyashio, and Kuroshio currents flow near the Sanriku coastline and control physical and biogeochemical processes in these coastal embayments (Ishizu et al. 2017, Tanaka et al. 2017). The supply of oceanic nutrients determines nutrient concentrations and affects primary production (Hayakawa 1990, Nakajima et al. 2021). A recent study of an embayment along the Sanriku ria coast revealed that nitrogen-enriched groundwater discharge, especially saline SGD, was a significant nutrient source in autumn, when offshore seawater intrusion was weak (Nakajima et al. 2021). Therefore, assessing the response of phytoplankton production to groundwater discharge relative to the effects of other nutrient sources is essential to elucidating biological production in coastal embayments along the Sanriku ria coast.

Based on our previous results (Nakajima et al. 2021), we hypothesized that nutrients derived from saline SGD are crucial to phytoplankton primary production. To clarify the influence of groundwater discharge on phytoplankton primary production, we conducted field experiments in the inner part of Kesennuma Bay (Fig. 1) along the Sanriku ria coast in summer and autumn, which have contrasting offshore seawater influences. First, phytoplankton primary productivity (PP) in surface seawater from the bay head to outside the bay was measured using the stable carbon isotope (^{13}C) tracer method and compared to the relative contribution of saline groundwater to surface nutrients quantified using a water source mixing model. Then, we determined the limiting nutrient (nitrogen, phosphorus, or silica) using a bioassay incubation experiment. Finally, we assessed the impact of saline SGD on phytoplankton primary production.

2. MATERIALS AND METHODS

2.1. Study site

Moune Bay is a semi-enclosed embayment located in the inner part of Kesennuma Bay along the Sanriku ria coast, Japan (Fig. 1). The Nishi-Moune and Higashi-Moune rivers flow into the head of Moune Bay; annual mean river discharges of the Nishi-Moune and Higashi-Moune rivers are 1.5×10^3 and 3.2×10^3 m^3 d^{-1}, respectively (Nakajima et al. 2021). Fresh and saline SGD into Moune Bay, quantified by the combination of the hydrological method (Darcy's Law) and the radium (Ra) mass balance model, are approximately 17 m^3 d^{-1} (area-normalized groundwater flux: 3.7×10^{-2} m^3 m^{-2} d^{-1}) and 23 000 m^3 d^{-1} (14.0×10^{-2} m^3 m^{-2} d^{-1}), respectively (Nakajima et al. 2021).

2.2. Fieldwork

We conducted 2 field surveys in summer (9 Jun 2018) and autumn (31 Oct 2018), during which we collected surface seawater from 6 stations. We used a submersible pump to obtain large-volume samples for Ra isotopes analysis and a bucket to obtain small-volume samples for other analyses. At each station, water temperature and salinity were measured using a CTD profiler (RINKO-Profiler ASTD102 or AAQ 117; JFE Advantech). To evaluate the influence of saline groundwater on surface seawater, we used Ra

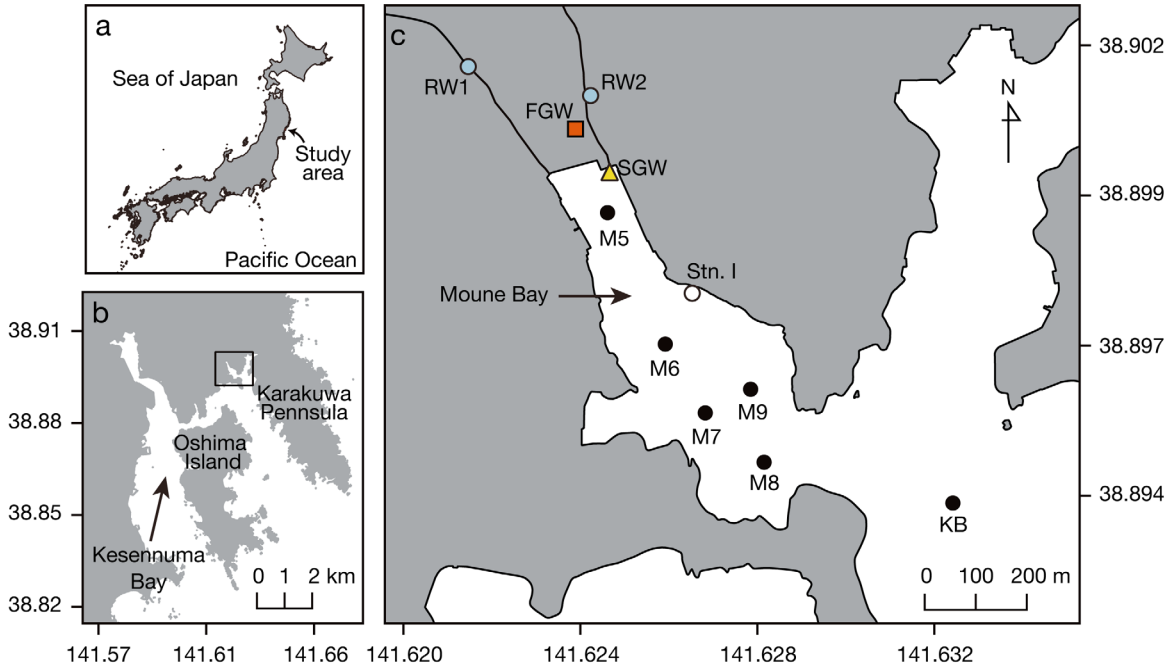

Fig. 1. (a,b) Study area. (c) Sampling locations. Black circles (Stns M5–M9, KB) indicate surface waters sampled for estimation of primary production and environmental parameters in 2018. White circle (Stn I) shows the location of surface seawater sampling for the bioassay incubation experiment in 2020. Blue circles, red square, and yellow triangle represent sampling stations of river water, fresh groundwater, and saline groundwater, respectively, used for the water source mixing model and the bioassay experiment

isotopes as a tracer for saline groundwater. We collected 60 to 70 l of seawater on MnO_2-impregnated acrylic fiber (Mn fiber) filters and analyzed the Ra isotopes to quantify the relative contribution of water sources to surface seawater. This was done using a mixing model analysis (see details in Section 2.4). The samples intended for nutrient analyses were immediately filtered through a syringe filter (cellulose-acetate membrane, 0.8 µm pore size; Advantec) into either 10 ml polystyrene bottles (for nitrate [NO_3^-], nitrite [NO_2^-], phosphate [PO_4^{3-}], and silicate [$Si(OH)_4$]) or 30 ml polyethylene bottles (for ammonium [NH_4^+]). The filtered samples were then stored at −25°C until analysis (≤5 mo for NO_3^-, NO_2^-, PO_4^{3-}, and $Si(OH)_4$ and ≤2 mo for NH_4^+). Filtrates intended for the analysis of dissolved inorganic carbon (DIC) concentration and its ^{13}C ratio ($\delta^{13}C$ of DIC) were stored in borosilicate vials with saturated mercury chloride solution and kept in a refrigerator at 4°C until analysis. Seawater passed through 100 µm nylon mesh was portioned into a 1 l polypropylene, a 2 l polypropylene, and three 500 ml polycarbonate incubation bottles at each station. The 1 l samples for the determination of the cell density of phytoplankton species through light microscopy were fixed with the addition of Lugol's iodine solution (10 ml) and stored in the dark in a refrigerator (4°C).

Water samples in the 2 l polypropylene bottles were transferred to the laboratory and kept in the dark until the next treatment. The samples were then filtered through pre-combusted glass fiber filters (GF/Fs; Whatman) within a few hours to determine chl *a* concentrations, particulate organic carbon (POC) concentrations, and $\delta^{13}C$ of POC. Samples for chl *a* and POC were obtained by filtering 100 to 150 ml and 200 to 500 ml, respectively, of water from a 2 l polypropylene bottle.

In the present study, we evaluated the photosynthetic rate using the procedure outlined by Hama et al. (1983). To examine phytoplankton primary production at each station and season, we added 1.2 ml of 0.1 M sodium bicarbonate ($NaH^{13}CO_3$) to three 500 ml polycarbonate bottles, representing approximately 10% of the total inorganic carbon content of ambient water (1921–2031 µmol l^{-1}; Table S1 in the Supplement at www.int-res.com/articles/suppl/m712p021_supp.pdf). These bottles were incubated for approximately 4 h during the daytime in a transparent flow-through water tank maintained at the same temperature as the surface seawater using a submersible pump. During the incubation experiments, photon flux and salinity and temperature were measured at 5 min intervals using a photon logger (DEFI; JFE Advantech) and a temperature and conductivity logger

(A7CT2-USB; JFE Advantech), respectively. After incubation, the water samples in the polycarbonate bottles were filtered through the Whatman GF/Fs for the analysis of POC concentration and $\delta^{13}C$ of POC.

2.3. Chemical analysis

NO_3^-, NO_2^-, PO_4^{3-}, and $Si(OH)_4$ concentrations were measured using an autoanalyzer (QuAAtro-2HR or QuAAtro 39; Bran-Luebbe). NO_2^- and NO_3^- concentrations were measured using the standard method of cadmium–copper reduction (Strickland & Parsons 1972), while PO_4^{3-} concentration was determined by the molybdenum blue method of Murphy & Riley (1962). Additionally, $Si(OH)_4$ concentration was measured using the molybdenum blue method of Hansen & Koroleff (1999). NH_4^+ concentration was measured fluorometrically using the ortho-phthaldialdehyde method (Holmes et al. 1999) with a fluorometer (Trilogy; Turner Designs). Total dissolved nitrogen (TDN) and total dissolved phosphorus (TDP) concentrations were measured using an autoanalyzer via wet oxidation with potassium persulfate. We defined dissolved inorganic nitrogen (DIN) as the sum of the NO_3^-, NO_2^-, and NH_4^+ concentrations; dissolved inorganic phosphorus (DIP) as PO_4^{3-}; and dissolved silica (DSi) as $Si(OH)_4$. Dissolved organic nitrogen (DON) and dissolved organic phosphorus (DOP) were calculated as the difference between TDN and DIN and between TDP and DIP, respectively. Detection limits for the analysis of nutrient concentrations, calculated as 3 times the SD of a blank measured during nutrient analysis, were 0.05 µmol l^{-1} for $NO_2^- + NO_3^-$, 0.07 µmol l^{-1} for NH_4^+, 0.04 µmol l^{-1} for PO_4^{3-}, and 0.19 µmol l^{-1} for $Si(OH)_4$. The GF/Fs used for chl *a* concentration analysis were extracted in the dark with 5 ml N,N-dimethylformamide (Suzuki & Ishimaru 1990) for over 12 h. Chl *a* concentration was measured using a calibrated fluorometer (Trilogy; Turner Designs) (Welschmeyer 1994). DIC concentrations were measured by acidifying and bubbling the samples and using a total organic carbon analyzer with nondispersive infrared CO_2 detection (TOC-V; Shimadzu) (Salonen 1981).

The analysis method used to measure the activities of ^{224}Ra and ^{228}Ra in Mn fiber is described in a companion work (Nakajima et al. 2021). Briefly, ^{224}Ra activity was analyzed using an Ra delayed coincidence counter (RaDeCC; Scientific Computer Instruments) (Moore & Arnold 1996) within 1 wk of the sampling date. To correct ^{224}Ra activities, we measured thorium isotopes (^{228}Th) in the Mn fibers 4 wk after the sampling date. ^{228}Ra activity was estimated through the measurement of ^{228}Th after a sufficient amount of time (>1 yr) had elapsed to produce distinguishable ^{228}Th from ^{228}Ra decay, according to a published equation (Moore 2008).

GF/Fs for natural and enriched ^{13}C analysis were placed overnight in a desiccator with HCl fumes to remove the inorganic carbon. These filters were analyzed using the Elementar vario EL cube or MICRO cube elemental analyzer (Elementar Analysensysteme) interfaced with the PDZ Europa 20-20 isotope ratio mass spectrometer (Sercon) at the University of California Davis Stable Isotope Facility. The analytical precision of $\delta^{13}C$ in natural and tracer samples was less than 0.1‰. $\delta^{13}C$ of DIC was measured using a GasBench II system interfaced to a stable isotope ratio mass spectrometer (GasBench II-Delta Plus XL; Thermo Fisher Scientific). Analytical precision was 0.1‰ for $\delta^{13}C$ of DIC. PP (µg C l^{-1} h^{-1}) was calculated following the method of Hama et al. (1983):

$$PP = (a_{is} - a_{ns}) / (a_{ic} - a_{ns}) \times POC / \Delta t \quad (1)$$

where a_{is} and a_{ns} are the atom % of ^{13}C of POC in the incubated and natural sample, respectively; a_{ic} is the atom % of ^{13}C of DIC; POC is the POC concentration (µg C l^{-1}) in the incubated sample; and Δt is the incubated time (h). Biomass-specific PP (P_B) was then calculated by normalizing PP to the chl *a* concentration.

2.4. Limiting factors for primary production

We assessed the factors limiting PP using the equations proposed by Steele (1962) for temperature (F_T) and light intensity (F_I) and the Michaelis-Menten equation for nutrients (F_N) as follows:

$$F_T = T/T_{opt} \times \exp(1 - T/T_{opt}) \quad (2)$$

$$F_I = I/I_{opt} \times \exp(1 - I/I_{opt}) \quad (3)$$

$$F_N = \min[DIN/(K_N + DIN), DIP/(K_P + DIP)] \quad (4)$$

where T_{opt} (25°C) and I_{opt} (419 µmol m^{-2} s^{-1}) represent the optimum temperature and light intensity, respectively, for phytoplankton growth. The half-saturation constants for DIN and DIP were determined to be K_N (= 1.7 µmol l^{-1}) and K_P (= 0.19 µmol l^{-1}), respectively, based on previous studies conducted along the Japanese coasts (Yanagi & Onitsuka 1999, Sugimoto et al. 2010). *T* and *I* were respectively set to the mean values of temperature and light in-

tensity observed during the incubation experiments, and the concentrations of DIN and DIP were determined based on the observed values at each station.

2.5. Mixing model analysis of surface seawater

We calculated the contribution of water sources using the Bayesian mixing model (SIMMR, version 0.4; Parnell 2016) in R 4.0.2 (R Core Team 2020). Although we used short-lived ^{224}Ra ($t_{1/2}$ = 3.66 d) and long-lived ^{228}Ra ($t_{1/2}$ = 5.75 yr) coupled with salinity (Fig. S1), the Ra activities of river water (RW) and fresh groundwater (FGW) were indistinguishable. In this study, we averaged the endmember values of RW and FGW as meteoric freshwater (FW) and thus considered the 3 endmembers of FW, saline groundwater (SGW), and offshore seawater (OW) in the mixing model analysis (Table S2). SGW was determined as the mean value of SGW collected at the tidal flat. Bottom seawater at Stn KB (Fig. 1c) was used as the endmember of offshore seawater. These values were obtained from a companion study (Table S2, Nakajima et al. 2021). The contribution rates of water sources are presented as the average value calculated from the salinity–^{224}Ra and salinity–^{228}Ra relationships. Finally, we estimated the contribution of each water source to the nutrient concentrations in surface seawater as follows:

$$f_{\mathrm{FW\text{-}N}} = \frac{f_{\mathrm{FW}} C_{\mathrm{FW}}}{f_{\mathrm{FW}} C_{\mathrm{FW}} + f_{\mathrm{SGW}} C_{\mathrm{SGW}} + f_{\mathrm{OW}} C_{\mathrm{OW}}} \quad (5)$$

$$f_{\mathrm{SGW\text{-}N}} = \frac{f_{\mathrm{SGW}} C_{\mathrm{SGW}}}{f_{\mathrm{FW}} C_{\mathrm{FW}} + f_{\mathrm{SGW}} C_{\mathrm{SGW}} + f_{\mathrm{OW}} C_{\mathrm{OW}}} \quad (6)$$

$$f_{\mathrm{OW\text{-}N}} = \frac{f_{\mathrm{OW}} C_{\mathrm{OW}}}{f_{\mathrm{FW}} C_{\mathrm{FW}} + f_{\mathrm{SGW}} C_{\mathrm{SGW}} + f_{\mathrm{OW}} C_{\mathrm{OW}}} \quad (7)$$

where $f_{\mathrm{FW\text{-}N}}$, $f_{\mathrm{SGW\text{-}N}}$, and $f_{\mathrm{OW\text{-}N}}$ are the contribution rates of FW, SGW, and OW, respectively, for each nutrient (DIN, DIP, and DSi); f_{FW}, f_{SGW}, and f_{OW} are the contribution rates of FW, SGW, and OW, respectively, estimated using the Bayesian mixing model; and C_{FW}, C_{SGW}, and C_{OW} are the mean concentrations to each nutrient (DIN, DIP, and DSi) from FW, SGW, and OW, respectively.

2.6. Bioassay experiment

To assess the nutrient limiting phytoplankton growth and determine whether groundwater inputs support primary production in Moune Bay, we conducted bioassay incubation experiments in summer (28 Jun–1 Jul 2020) and autumn (8–11 Nov 2020). An intermediate location between the bay head and bay mouth was chosen for the bioassay incubation experiments (Fig. 1c). Surface seawater (Stn I, Fig. 1c) was filtered using 100 µm nylon mesh and then stored temporally in acid-cleaned polyethylene Cubitainers for the bioassay experiments. To determine the phytoplankton species composition, we placed a water sample into a 1 l polypropylene bottle and added 10 ml of Lugol's iodine solution. RW, FGW, and SGW were taken from the 2 rivers (Nishi-Moune and Higashi-Moune), a shallow well, and a tidal flat, respectively (Fig. 1c). We mixed the RW samples on a vol/vol basis using the ratio of annual mean discharge of the Nishi-Moune River (1.5×10^3 m^3 d^{-1}) and the Higashi-Moune River (3.2×10^3 m^3 d^{-1}), which is 1:2.2 (Nakajima et al. 2021). The RW, FGW, and SGW samples were filtered through Whatman GF/Fs and stored in an acid-cleaned container at 4°C until the incubation experiment.

After water sampling, we immediately dispensed the seawater samples (<100 µm) into acid-cleaned 300 ml clear polypropylene bottles (triplicates per treatment) and finally prepared 12 treatments (no NH_4^+ treatment) in summer and 13 treatments in autumn (Fig. S2). Then, nutrients, RW, FGW, and SGW were added to each incubation bottle except the control. Nutrient treatments included NO_3^- (NO3; NO_3^- = 33 µmol l^{-1}), NH_4^+ (NH4; NH_4^+ = 15 µmol l^{-1}), PO_4^{3-} (P; PO_4^{3-} = 1 µmol l^{-1}), $Si(OH)_4$ (Si; $Si(OH)_4$ = 150 µmol l^{-1}), NO3+P (NO_3^- = 33 µmol l^{-1} and PO_4^{3-} = 1 µmol l^{-1}), and NO3+Si (NO_3^- = 33 µmol l^{-1} and $Si(OH)_4$ = 150 µmol l^{-1}). These treatments were spiked through the addition of approximately 10 times the nutrient concentration of surface seawater in Moune Bay to induce strong growth responses of phytoplankton. For the RW, FGW, and SGW treatments, we spiked RW, FGW, and SGW at 5 and 10% of the bottle volume. To elicit a phytoplankton response within the 3 d incubation period following the method of Lecher et al. (2015), we added slightly more RW, FGW, and SGW to the treatment bottles than the contributions of each water source to surface seawater identified by the mixing model analysis (Table S3). Then, the incubation bottles were set in a flow-through tank filled with surface seawater (Fig. S2). During the incubation experiments, photon flux density and temperature were measured at 5 min intervals using a photon logger (DEFI2-L; JFE Advantech) and a conductivity and temperature recorder (DEFI2-CT; JFE Advantech), respectively. We took samples

after 0, 24, 48, and 72 h for measurement of chl *a* and nutrient concentrations (Fig. S2).

GF/Fs for the analysis of chl *a* concentration were extracted over 12 h in the dark with 5 ml N,N-dimethylformamide, and chl *a* concentration was measured using a calibrated fluorometer (Trilogy; Turner Designs). Nutrient concentration was measured using an autoanalyzer (QuAAtro 39; Bran-Luebbe) (see details in Section 2.3).

2.7. Statistical analyses

We used 2-sample tests to test the significance of the difference in phytoplankton parameters (PP, chl *a* concentration, and P_B) and contribution of each source (FW, SGW, and OW) between summer and autumn. To test the homogeneity of variances prior to the 2-sample test, we applied Levene's test with a significance level of $\alpha = 0.05$. When the result of the Levene's test was significant or not, a robust Brunner-Munzel test or Mann-Whitney *U*-test, respectively, was used, with a significance level of $\alpha = 0.05$ for both tests.

The differences in chl *a* concentrations among the various treatments from the bioassay experiments were analyzed by 1-way ANOVA, followed by a Tukey's HSD test ($p < 0.05$).

3. RESULTS AND DISCUSSION

3.1. Primary production and water sources in surface seawater

CTD observations showed prominent physical differences between the 2 seasons (Fig. S3). In summer, the surface water had higher temperature (>18°C) and lower salinity (≤31), and a prominent pycnocline was observed in the upper layer. In contrast, in autumn, the water was well mixed with higher salinity (≥33).

PP in surface seawater evaluated using the ^{13}C tracer method ranged from 7.4 to 24.3 µg C l^{-1} h^{-1} with a median (± quartile deviation [QD]) of 17.5 ± 4.0 µg C l^{-1} h^{-1} in summer and from 17.1 to 34.6 µg C l^{-1} h^{-1} with a median of 25.4 ± 3.1 µg C l^{-1} h^{-1} in autumn (Fig. 2a). These values were considerably higher than PP estimated using the same ^{13}C tracer method at other embayments (i.e. Onagawa Bay, Otsuchi Bay, and Kamaishi Bay) along the Sanriku ria coast (Shiozaki et al. 2020). This difference may be due to the coastal environment of this study site, which is more enclosed and likely to be influenced by land-derived nutrients than the other embayments. Although no significant seasonal difference was found in PP values (Mann-Whitney *U*-test, $p = 0.06$), chl *a* concentrations and P_B values showed signifi-

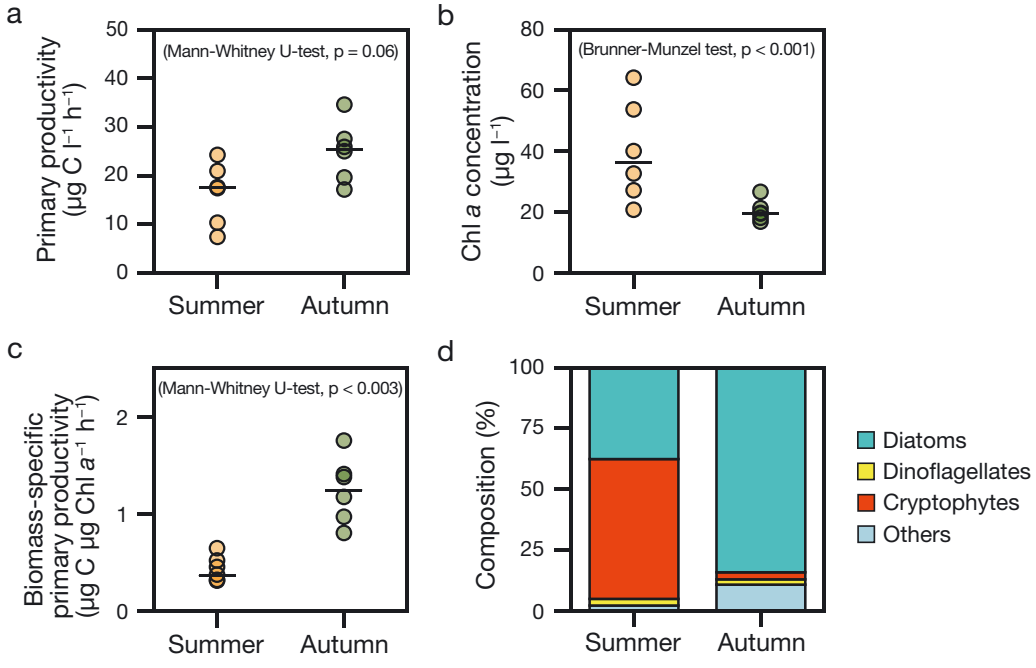

Fig. 2. (a) Primary productivity, (b) chl *a* concentration, (c) biomass-specific primary productivity, and (d) phytoplankton composition in summer and autumn 2018. Circles indicate observed values at each sampling site, and horizontal bars show the median values. Phytoplankton composition is expressed as mean values of the 6 sites. Based on the homogeneity of variances (Levene's test), the Mann-Whitney *U*-test or Brunner-Munzel test was used to test differences between summer and autumn

cant seasonal differences (Mann-Whitney *U*-test or Brunner-Munzel test, $p < 0.003$) (Fig. 2b,c). The median values (±QD) of chl *a* concentrations were significantly higher in summer (36.4 ± 10.9 µg l^{-1}) than in autumn (19.6 ± 1.2 µg l^{-1}) (Fig. 2b). However, the median P_B values were significantly lower in summer (0.4 ± 0.1 µg C µg chl a^{-1} h^{-1}) than in autumn (1.2 ± 0.2 µg C µg chl a^{-1} h^{-1}) (Fig. 2c).

Nutrient concentrations differed considerably between seasons (Table S1). Nutrients in summer were characterized by lower concentrations of DIN (0.9 ± 0.3 µmol l^{-1}, median ± QD) and DIP (0.04 ± 0.00 µmol l^{-1}) and higher concentrations of DSi (67.2 ± 38.1 µmol l^{-1}) compared to autumn. In contrast, samples taken in autumn showed higher concentrations of DIN (3.7 ± 0.4 µmol l^{-1}) and DIP (0.14 ± 0.02 µmol l^{-1}) but lower concentrations of DSi (9.8 ± 1.4 µmol l^{-1}). Considering that DSi concentration is often depleted when diatoms dominate the phytoplankton community due to their high demand for silicon (Conley & Malone 1992, Cloern et al. 2017), the significant contribution of diatoms to the phytoplankton community in autumn suggests a potential depletion of DSi in this season due to biological demand. Because diatoms have an ability to more easily take up nutrients and have a high photosynthesis rate under nutrient-enriched conditions compared to other phytoplankton species (Lomas & Glibert 2000, Sarthou et al. 2005, Marañón 2015), higher nutrient (i.e. DIN and DIP) concentrations in autumn also indicate that high P_B values in autumn (Fig. 2c) may be linked to the high proportion of diatoms in the phytoplankton composition (84% diatoms) compared to summer (57% cryptophytes, 38% diatoms) (Fig. 2d). The ratios of DIN:DIP (median N:P = 23.0 in summer and 26.8 in autumn) and DIN:DSi (median N:Si < 0.5) were higher and lower, respectively, than the Redfield ratio (N:P:Si = 16:1:15; Redfield et al. 1963, Brzezinski 1985). These ratios did not differ significantly between summer and autumn (Mann-Whitney *U*-test, $p = 0.48$). Furthermore, the incubation experiments using the ^{13}C tracer method indicated that nutrient concentration was the primary limiting factor for phytoplankton primary production in both seasons, as shown by the lowest F_N values compared to F_T and F_I (Table S4). As the nutrient molar ratio (N:P:Si) in seawater reflects the limiting nutrient for phytoplankton growth (Fisher et al. 1992, Burson et al. 2016), our results suggest that phosphorus was apparently limited relative to available amounts of nitrogen and silica for phytoplankton primary production in both seasons. Therefore, phosphorus availability might be crucial for phytoplankton primary production.

The contributions of SGW to each nutrient differed considerably between summer and autumn (Fig. 3). The median contribution of SGW to DIN, DIP, and DSi concentrations in autumn were 38.3, 19.0, and 21.0%, respectively. These concentrations were considerably higher than those observed in summer (19.3% for DIN, 7.1% for DIP, and 12.7% for DSi) (Mann-Whitney *U*-test, $p < 0.02$). Corresponding to the high contribution of SGW in autumn, DIN and DIP derived from SGW showed higher concentrations in autumn than in summer, but DSi did not. Notably, P_B values showed positive correlations with the contribution of SGW to all nutrients ($r \geq 0.64$, $p \leq 0.02$; Fig. 4c), although chl *a* concentration showed a negative correlation with the contribution rate of SGW ($r \geq -0.74$, $p \leq 0.006$; Fig. 4b). These results may suggest that increased nutrient inputs derived from SGW can be the source of high PP in surface seawater.

Meanwhile, the contribution rates of FW (9.0% for DIN, 3.6% for DIP, and 18.7% for DSi) and OW (52.9% for DIN, 77.5% for DIP, and 60.6% for DSi) in autumn were lower (~0.6 times) or comparable (~1.2 times) to rates in summer. The median value of OW contribution exceeds 50% in both seasons (Fig. 3), indicating that OW-derived nutrients were a primary component of nutrients in surface seawater. In particular, OW-derived DIP concentration was high in autumn (Fig. 3e). The positive correlation of OW contributions to DIN and DIP with chl *a* concentrations ($r = 0.67$, $p = 0.02$; Fig. S4b) suggests that the biomass of phytoplankton might be controlled by the influence of oceanic water. Similar results have been obtained from several coasts (e.g. Sugimoto et al. 2010, Watanabe et al. 2017). The RW contribution to DSi was negatively correlated with PP and P_B ($r \leq -0.59$, $p < 0.05$; Fig. S5).

3.2. Limiting nutrients for phytoplankton growth

The initial and incubation conditions of the bioassay experiments are listed in Table 1. Photon fluxes during the bioassay incubation did not differ with season, although the water temperature was approximately 4°C higher in summer than in autumn. DIN and DSi concentrations in summer (2.29 µmol l^{-1} for DIN and 9.53 µmol l^{-1} for DSi) were comparable to those in autumn (3.15 µmol l^{-1} for DIN and 8.19 µmol l^{-1} for DSi). Meanwhile, DIP concentration was near the detection limit (0.04 µmol l^{-1}) in summer and increased to 0.27 µmol l^{-1} in autumn. The limiting factor values for phytoplankton growth, calcu-

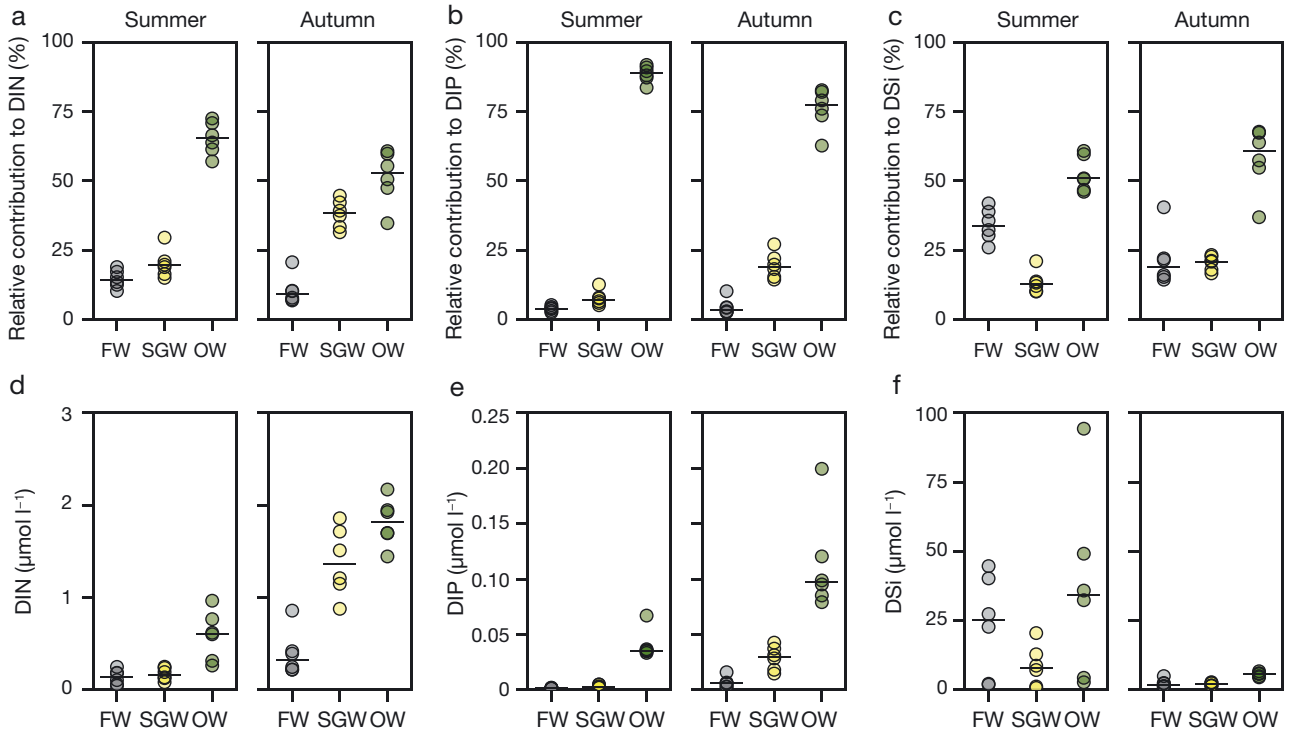

Fig. 3. Seasonal differences in the contribution and calculated concentrations of dissolved inorganic nitrogen (DIN), dissolved inorganic phosphorus (DIP), and dissolved silica (DSi) derived from meteoric freshwater (FW: river water + fresh groundwater), saline groundwater (SGW), and offshore seawater (OW) in 2018. Circles represent estimated values at each sampling site, and horizontal bars show the median values of the 6 sites

lated using Eqs. (2–4), showed that nutrient concentration was the primary limiting factor for phytoplankton primary production in both seasons, as shown by the lowest F_N values (≤0.59) compared to F_T (≥0.90) and F_I (= 0.85). DIN:DIP:DSi molar ratios differed considerably between summer (= 52:1:216) and autumn (= 12:1:30). Based on the Redfield ratio (Redfield et al. 1963, Brzezinski 1985), the nutrient environment of the incubation experiment was likely to be under phosphorus limitation in summer and slight nitrogen limitation in autumn. Despite lower chl *a* concentrations (t = 0) in both seasons in 2020 compared to those in 2018 (Figs. 2 & 5), the dominant phytoplankton groups were similar between the 2 years (Tables 1 & S1).

The nutrient addition bioassay experiments showed the most significant increase in chl *a* concentration with the NO3+P treatment in both seasons ($p < 0.05$; Fig. 5). The nitrogen addition (NO3, NH4, and NO3+Si) also showed a significant increase in chl *a* concentration ($p < 0.05$), except for the NO3+Si treatment in autumn ($p > 0.05$; Fig. 5b). Chl *a* concentrations in other treatments (P, Si) did not increase significantly ($p < 0.05$; Fig. 5). These results revealed that nitrogen, rather than phosphorus, was the primary nutrient limiting phytoplankton growth in both seasons. Nitrogen limitation has been reported in other embayments along the Sanriku ria coast (Ohara et al. 2018, Shiozaki et al. 2020). The bioassay experiment in summer indicated that nitrogen was the limiting nutrient for phytoplankton growth (i.e. N; Fig. 5), whereas the molar ratios of nutrients in surface seawater suggested phosphorus as the limiting nutrient (i.e. P, DIN:DIP:DSi = 52:1:216) (Table 1). This contradiction suggests that the nutrient molar ratio in seawater might not be an adequate indicator of the limiting nutrient for phytoplankton growth, as noted in previous studies (Tamminen & Andersen 2007, Trommer et al. 2013, Turner & Rabalais 2013, Hidaka et al. 2022). Therefore, even though phosphorus was lower than the nutrient molar ratio (Table S1), the results imply that phytoplankton growth in both seasons in 2018 might have been limited by nitrogen.

The bioassay experiment showed that phytoplankton growth responds to nitrogen addition under DIP-depleted conditions in summer. This contradiction may be due to cryptophytes dominating the phytoplankton community in summer (= 58%) (Table 1). Cryptophytes are mixotrophic species that can obtain phosphorus from bacteria through phagocytosis when phosphorus is limited (Unrein et al. 2007). Furthermore, the availability of DOP as the phosphorus source may be an important factor. The 2 bioassay treatments (control, NO3) showed a significant

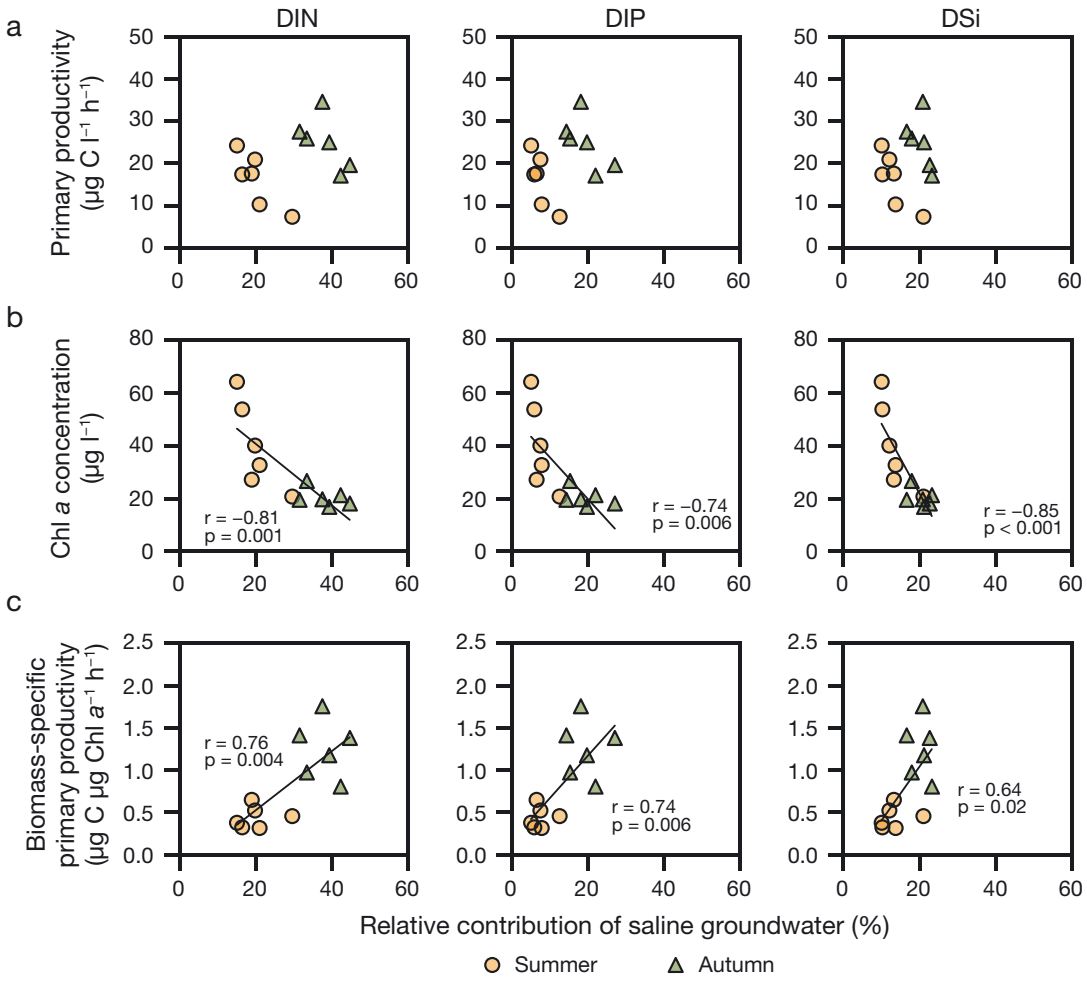

Fig. 4. Saline groundwater contributions to nutrients relative to (a) primary productivity, (b) chl *a* concentrations, and (c) biomass-specific primary productivity in 2018. Circles and triangles indicate observed values at each sampling station in summer and autumn, respectively

decrease in DOP concentration (approx. −17%) in summer ($p < 0.05$; Fig. S6f), while most treatments except for NO3, Si, and NO3+Si showed a significant increase in DOP concentration (approx. +318%) in autumn ($p < 0.05$; Fig. S6l). Phytoplankton may obtain their phosphorus requirements from the DOP pool (e.g. Dyhrman & Ruttenberg 2006, Mahaffey et al. 2014, Martin et al. 2014) as well as nitrogen requirements from the DON pool (e.g. Bronk et al. 2007, Korth et al. 2012). These results imply that the availability of phosphorus except for DIP in seawater could result in nitrogen-limited conditions for phytoplankton growth.

Phytoplankton growth showed a prominent response to additions of RW, FGW, and SGW (Fig. 5a,b). The 10% RW, FGW, and SGW treatments increased chl *a* concentration during both seasons ($p < 0.05$; Fig. 5), while the 5% FGW and SGW treatments showed a significant increase in chl *a* concentrations only in autumn ($p < 0.05$; Fig. 5b). Regardless of season, DIN and DSi concentrations in each water sample were respectively ≥5.9 and ≥11.2 times higher than their concentrations in surface seawater (Fig. 6, Tables 1 & S5). In addition, the DIN:DIP ratios of RW, FGW, and SGW were above the Redfield ratio (N:P ≥71 for RW, ≥76 for FGW, ≥45 for SGW). As phytoplankton growth was primarily limited by nitrogen availability in both seasons (Fig. 5), inputs of nitrogen-enriched FW and SGW could be essential, mitigating the nitrogen limitation of primary production.

3.3. Significance of saline SGD for primary production

In Moune Bay, the discharge of SGW is the most significant nutrient source from the land–sea boundary (RW + FGW + SGW) to the bay based on volumetric assessment of DIN, DIP, and DSi fluxes (Nakajima et al. 2021). In this study, we found that higher P_B

Table 1. Initial and incubation conditions of bioassay experiments in 2020 (error terms are SD). NO_2^-: nitrite; NO_3^-: nitrate; NH_4^+: ammonium; DIN: dissolved inorganic nitrogen; DIP: dissolved inorganic phosphorus; DSi: dissolved silica

	Summer	Autumn
Period	28 Jun–1 Jul 2020	8–11 Nov 2020
Incubation condition (mean ± SD)		
Temperature (°C)	19.7 ± 1.7	15.3 ± 0.7
Photon flux (µmol m^{-2} s^{-1})	220.7 ± 366.1	222.0 ± 383.4
Initial condition		
Temperature (°C)	19.6	17.3
Salinity	31.90	32.50
NO_2^- + NO_3^- (µmol l^{-1})	0.89	2.38
NH_4^+ (µmol l^{-1})	1.40	0.77
DIN (µmol l^{-1})	2.29	3.15
DIP (µmol l^{-1})	0.04	0.27
DSi (µmol l^{-1})	9.53	8.19
DIN:DIP:DSi	52:1:216	12:1:30
Chl *a* (µg l^{-1})	1.8 ± 0.1	1.5 ± 0.1
Phytoplankton density (×10^2 cells ml^{-1})	3.7	3.7
Phytoplankton composition (%)		
Diatoms	2	45
Dinophytes	<1	<1
Cryptophytes	58	17
Prasinophytes	5	11
Others	35	26

values in autumn were sustained by higher contributions of SGW to nutrient concentrations (Fig. 4). This finding may be attributed to the nitrogen supply from SGW for mitigating the nitrogen limitation of phytoplankton growth in addition to the dominance of diatoms with an ability to have a high photosynthesis rate under nutrient-enriched conditions (Table 1). Although the supply of oceanic nutrients dominates the nutrient environment in Moune Bay (Nakajima et al. 2021), an additional supply of nitrogen-enriched SGW (Fig. 6, Table S5) may enhance phytoplankton growth in the nitrogen-limited seawater in Moune Bay. Similarly, Lecher et al. (2015) reported that nitrogen-enriched SGW promoted phytoplankton growth under nitrogen-limited conditions in Monterey Bay. The importance of recirculated SGD for phytoplankton primary production has also been reported along the nearshore

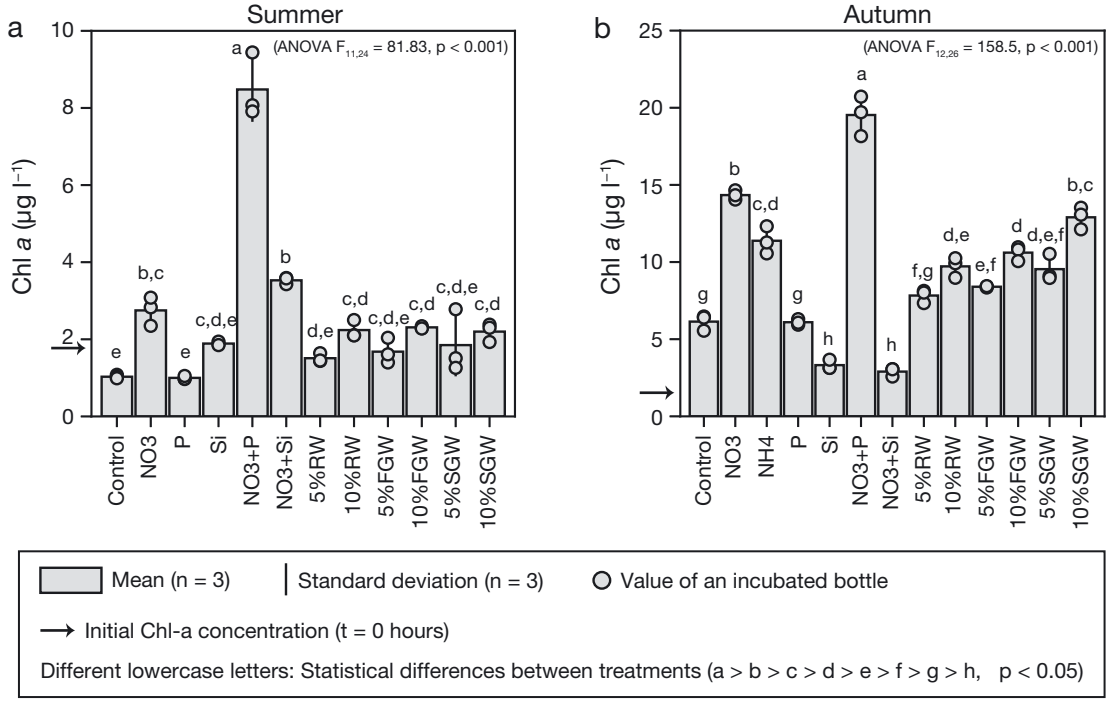

Fig. 5. Chl *a* concentrations at the end of incubation (*t* = 72 h) in each treatment of nutrient, river water (RW), fresh groundwater (FGW), and saline groundwater (SGW) experiments in 2020. Bars indicate the mean values of triplicate samples (circles). Labels with the different letters above bars indicate statistically different mean chl *a* concentrations between treatments (a > b > c > d > e > f > g > h; ANOVA followed by a Tukey's HSD test, p <0.05), whereas labels with the same letters above bars indicate no statistically different mean chl *a* concentrations between treatments. Arrows represent initial chl *a* concentrations (*t* = 0 h)

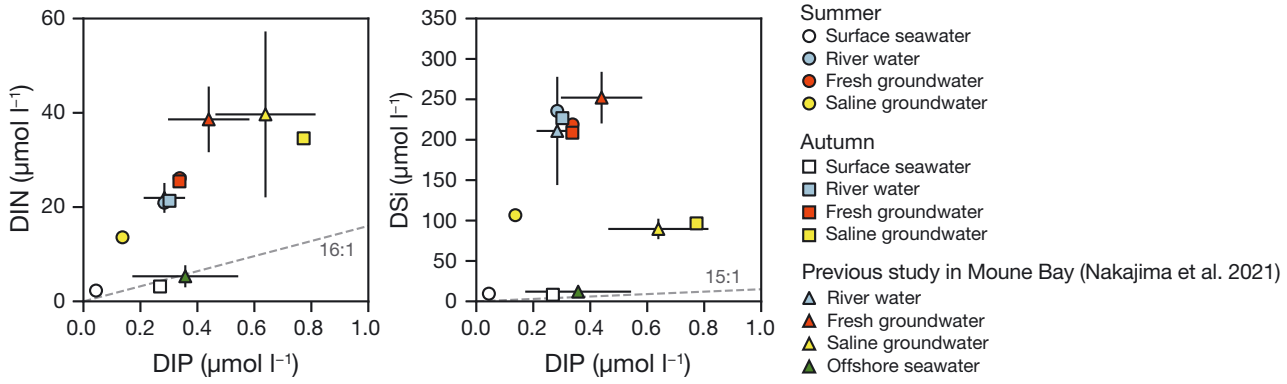

Fig. 6. Nutrient properties of surface seawater, river water, fresh groundwater, and saline groundwater used in the bioassay experiments in 2020. Triangles represent nutrient concentrations of endmembers reported in previous research in Moune Bay (Nakajima et al. 2021). Error bars show the 95% CI of each source. Dashed line represents the Redfield ratio (Redfield 1963, Brzezinski 1985). DIN: dissolved inorganic nitrogen; DIP: dissolved inorganic phosphorus; DSi: dissolved silica

coast of Obama Bay (Kobayashi et al. 2017, Sugimoto et al. 2017). Therefore, we can conclude that SGW is volumetrically important and is a crucial nitrogen source for phytoplankton primary production within the bay.

However, other factors that may control phytoplankton production and phytoplankton species composition must also be considered. The higher PP observed in autumn was mainly driven by diatoms (Fig. 2). The increase in primary production with SGW input is related to diatom abundance, as this group effectively assimilates nitrogen (Lecher et al. 2017). However, physical conditions and oceanic nutrient supply have non-negligible effects on phytoplankton primary production in surface seawater. Surface seawater in autumn had higher concentrations and contributions of offshore DIN and DIP compared to summer (Fig. 3), although Nakajima et al. (2021) reported that nutrient flux from offshore seawater to Moune Bay in autumn was lower than that in summer. These results imply that vertical mixing in autumn (Fig. S3) might promote the supply of offshore nutrients to surface waters and accelerate phytoplankton primary production even if there is a lower flux of oceanic nutrients. Although the bioassay experiment revealed that the addition of phosphorus did not stimulate phytoplankton growth, the growth was highest in the co-addition treatment of nitrogen and phosphorus among all other treatments (Fig. 5). Therefore, the effectiveness of nitrogen supply from SGW for supporting the primary production of diatoms would be maximized under DIP-enriched conditions, which are present in surface seawater in autumn.

As the bioassay experiments showed, the most significant response of phytoplankton to the combined NO3+P treatment in both seasons ($p < 0.05$; Fig. 5), the contribution of nitrogen derived from saline groundwater to primary production would vary with changes in coastal environmental conditions (i.e. P depleted or P enriched) (Fig. 7). Under phosphorus-depleted conditions, the nitrogen supply from SGW must be essential to mitigating the nitrogen limita-

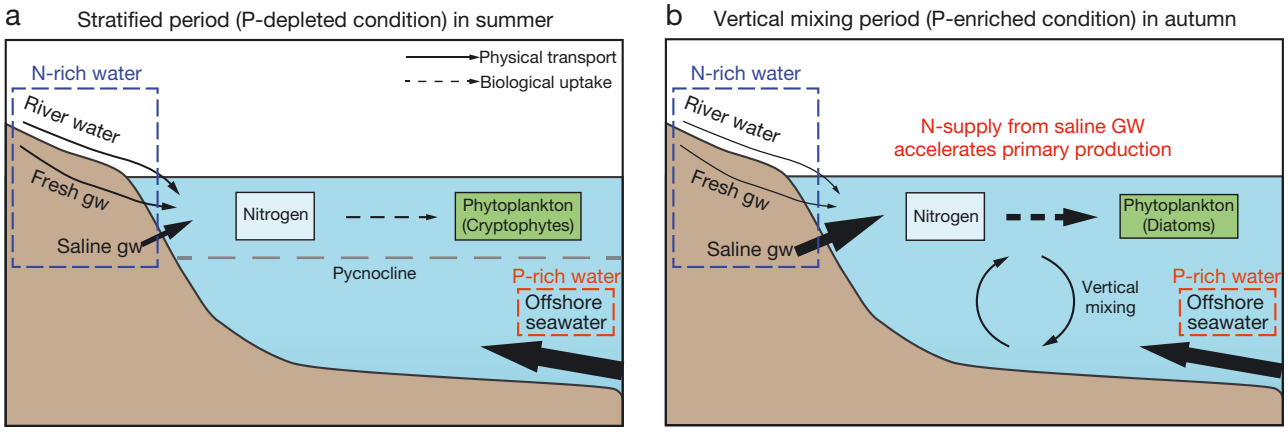

Fig. 7. Impact of nitrogen-enriched saline groundwater on primary production in surface seawater in Moune Bay during (a) the summer stratified period and (b) the autumn vertical mixing period

tion of phytoplankton growth, although the dominance of mixotrophic cryptophytes complicates the assessment of SGW discharge (Fig. 7a). Given that nitrogen additions have been shown to increase alkaline phosphatase activity in organisms such as phytoplankton and bacteria (e.g. Ruttenberg & Dyhrman 2012, Mahaffey et al. 2014), the nitrogen input from SGW in low phosphorus conditions could play a dual role in sustaining phytoplankton primary production by providing both direct nutrients for cell growth and indirect pathways such as enhancing alkaline phosphatase activity and facilitating cascading effects between bacteria and mixotrophic species (Lecher & Mackey 2018). Conversely, in autumn, SGW discharge greatly accelerates phytoplankton primary production under conditions of weak stratification and phosphorus enrichment (Fig. 7b).

4. CONCLUSIONS

We assessed the effect of nutrient input from SGW on phytoplankton primary production in contrasting offshore nutrient supply conditions during summer (stratified condition) and autumn (vertical mixed condition). Water source analyses based on Ra isotopes revealed the relative contribution of SGW to concentrations of DIN (19.3–38.3%), DIP (7.1–19.0%), and DSi (12.7–21.0%) in surface seawater. Higher P_B was observed in autumn when the relative contribution of SGW increased, indicating that nutrients derived from SGW can be the source of high PP. Bioassay experiments in both seasons revealed that the most significant phytoplankton response was observed in the combination of nitrogen and phosphorus. Nitrogen treatment alone also showed enhancement in phytoplankton response, while no response was observed in the phosphorus and silica treatments. Therefore, we conclude that SGW-derived nitrogen could stimulate phytoplankton growth and can be more effective for phytoplankton primary production under the high contribution of offshore phosphorus to surface water in the vertically mixed season. While the importance of SGD on phytoplankton primary production may vary depending on the site, the significance of SGD for biological production in coastal seas worldwide is undeniable.

Acknowledgements. We thank Mr. Makoto Hatakeyama of NPO Mori-Umi and members of the Faculty of Marine Biosciences and Technology, Fukui Prefectural University, for their assistance in the field experiment. Nutrient analysis was partly conducted at the Maizuru Fisheries Research Station, Field Science Education and Research Center, Kyoto University. This work was supported by the Japan Society for the Promotion of Science (JSPS), KAKENHI Grant Nos. 16H06200, 18KK0428, 18H03799, 20J23471, 21H02271, and 22H05202.

LITERATURE CITED

Ara K, Yamaki K, Wada K, Fukuyama S and others (2011) Temporal variability in physicochemical properties, phytoplankton standing crop and primary production for 7 years (2002–2008) in the neritic area of Sagami Bay, Japan. J Oceanogr 67:87–111

Brett MT, Kainz MJ, Taipale SJ, Seshan H (2009) Phytoplankton, not allochthonous carbon, sustains herbivorous zooplankton production. Proc Natl Acad Sci USA 106:21197–21201

Bronk DA, See JH, Bradley P, Killberg L (2007) DON as a source of bioavailable nitrogen for phytoplankton. Biogeosciences 4:283–296

Brzezinski MA (1985) The Si:C:N ratio of marine diatoms: interspecific variability and the effect of some environmental variables. J Phycol 21:347–357

Burson A, Stomp M, Akil L, Brussaard CPD, Huisman J (2016) Unbalanced reduction of nutrient loads has created an offshore gradient from phosphorus to nitrogen limitation in the North Sea. Limnol Oceanogr 61:869–888

Cabral A, Sugimoto R, Taniguchi M, Tait D, Nakajima T, Honda H, Santos IR (2023) Fresh and saline submarine groundwater discharge as sources of carbon and nutrients to the Japan Sea. Mar Chem 249:104209

Chassot E, Bonhommeau S, Dulvy NK, Mélin F, Watson R, Gascuel D, Le Pape O (2010) Global marine primary production constrains fisheries catches. Ecol Lett 13: 495–505

Cloern JE (1991) Annual variations in river flow and primary production in the south San Francisco Bay Estuary (USA). In: Elliott M, Ducrotoy JP (eds) Estuaries and coasts: spatial and temporal intercomparisons. Olsen & Olsen, Fredensborg, p 91–96

Cloern JE, Jassby AD, Schraga TS, Nejad E, Martin C (2017) Ecosystem variability along the estuarine salinity gradient: examples from long-term study of San Francisco Bay. Limnol Oceanogr 62:S272–S291

Conley DJ, Malone TC (1992) Annual cycle of dissolved silicate in Chesapeake Bay: implications for the production and fate of phytoplankton biomass. Mar Ecol Prog Ser 81:121–128

Diego-Feliu M, Rodellas V, Alorda-Kleinglass A, Saaltink M, Folch A, Garcia-Orellana J (2022) Extreme precipitation events induce high fluxes of groundwater and associated nutrients to coastal ocean. Hydrol Earth Syst Sci 26: 4619–4635

Dyhrman ST, Ruttenberg KC (2006) Presence and regulation of alkaline phosphatase activity in eukaryotic phytoplankton from the coastal ocean: implications for dissolved organic phosphorus remineralization. Limnol Oceanogr 51:1381–1390

Falkowski PG, Barber RT, Smetacek VV (1998) Biogeochemical controls and feedbacks on ocean primary production. Science 281:200–207

Field CB, Behrenfeld MJ, Randerson JT, Falkowski P (1998) Primary production of the biosphere: integrating terrestrial and oceanic components. Science 281:237–240

Fisher TR, Peele ER, Ammerman JW, Harding LW (1992)

Nutrient limitation of phytoplankton in Chesapeake Bay. Mar Ecol Prog Ser 82:51–63
Furuya K, Takahashi K, Iizumi H (1993) Wind-dependent formation of phytoplankton spring bloom in Otsuchi Bay, a ria in Sanriku, Japan. J Oceanogr 49:459–475
Hama T, Miyazaki T, Ogawa Y, Iwakuma T, Takahashi M, Otsuki A, Ichimura S (1983) Measurement of photosynthetic production of a marine phytoplankton population using a stable ^{13}C isotope. Mar Biol 73:31–36
Hansen HP, Koroleff F (1999) Determination of nutrients. In: Grasshoff K, Kremling K, Ehrhardt M (eds) Methods of seawater analysis, 3rd edn. Wiley-VCH, Weinheim, p 159–228
Hayakawa Y (1990) Mean seasonal changes of dissolved inorganic nutrients in the Ofunato Estuary. Bull Jpn Soc Sci Fish 56:1717–1729
Hidaka R, Nishiyama K, Yoshino K, Yasui-Tamura S, Hashihama F, Katano T (2022) Nutrient limitation on phytoplankton growth and abundance in the innermost area of Tokyo Bay. Bull Coastal Oceanogr 2022.11.001 (in Japanese with English abstract)
Holmes RM, Aminot A, Kérouel R (1999) A simple and precise method for measuring ammonium in marine and freshwater ecosystems. Can J Fish Aquat Sci 56: 1801–1808
Ishizu M, Itoh S, Tanaka K, Komatsu K (2017) Influence of the Oyashio Current and Tsugaru Warm Current on the circulation and water properties of Otsuchi Bay, Japan. J Oceanogr 73:115–131
Jickells TD (1998) Nutrient biogeochemistry of the coastal zone. Science 281:217–221
Johannes RE (1980) The ecological significance of the submarine discharge of groundwater. Mar Ecol Prog Ser 3: 365–373
Kobayashi S, Fujiwara T (2008) Long-term variability of shelf water intrusion and its influence on hydrographic and biogeochemical properties of the Seto Inland Sea, Japan. J Oceanogr 64:595–603
Kobayashi S, Sugimoto R, Honda H, Miyata Y and others (2017) High-resolution mapping and time-series measurements of ^{222}Rn concentrations and biogeochemical properties related to submarine groundwater discharge along the coast of Obama Bay, a semi-enclosed sea in Japan. Prog Earth Planet Sci 4:6
Korth F, Deutsch B, Liskow I, Voss M (2012) Uptake of dissolved organic nitrogen by size-fractionated plankton along a salinity gradient from the North Sea to the Baltic Sea. Biogeochemistry 111:347–360
Lecher AL, Mackey KRM (2018) Synthesizing the effects of submarine groundwater discharge on marine biota. Hydrology 5:60
Lecher AL, Mackey K, Kudela R, Ryan J, Fisher A, Murray J, Paytan A (2015) Nutrient loading through submarine groundwater discharge and phytoplankton growth in Monterey Bay, CA. Environ Sci Technol 49:6665–6673
Lecher AL, Mackey KRM, Paytan A (2017) River and submarine groundwater discharge effects on diatom phytoplankton abundance in the Gulf of Alaska. Hydrology 4: 61
Liang W, Liu Y, Jiao JJ, Luo X (2020) The dynamics of dissolved inorganic nitrogen species mediated by fresh submarine groundwater discharge and their impact on phytoplankton community structure. Sci Total Environ 703:134897
Liefer JD, MacIntyre HL, Novoveská L, Smith WL, Dorsey CP (2009) Temporal and spatial variability in *Pseudonitzschia* spp. in Alabama coastal waters: a 'hot spot' linked to submarine groundwater discharge? Harmful Algae 8:706–714
Lomas MW, Glibert PM (2000) Comparisons of nitrate uptake, storage, and reduction in marine diatoms and flagellates. J Phycol 36:903–913
Mahaffey C, Reynolds S, Davis CE, Lohan MC (2014) Alkaline phosphatase activity in the subtropical ocean: insights from nutrient, dust and trace metal addition experiments. Front Mar Sci 1:73
Marañón E (2015) Cell size as a key determinant of phytoplankton metabolism and community structure. Annu Rev Mar Sci 7:241–264
Martin P, Dyhrman ST, Lomas MW, Poulton NJ, Van Mooy BAS (2014) Accumulation and enhanced cycling of polyphosphate by Sargasso Sea plankton in response to low phosphorus. Proc Natl Acad Sci USA 111:8089–8094
Moore WS (2008) Fifteen years experience in measuring ^{224}Ra and ^{223}Ra by delayed-coincidence counting. Mar Chem 109:188–197
Moore WS, Arnold R (1996) Measurement of ^{223}Ra and ^{224}Ra in coastal waters using a delayed coincidence counter. J Geophys Res 101:1321–1329
Murphy J, Riley JP (1962) A modified single solution method for the determination of phosphate in natural waters. Anal Chim Acta 27:31–36
Nakajima T, Sugimoto R, Tominaga O, Takeuchi M, Honda H, Shoji J, Taniguchi M (2018) Fresh and recirculated submarine groundwater discharge evaluated by geochemical tracers and a seepage meter at two sites in the Seto Inland Sea, Japan. Hydrology 5:61
Nakajima T, Sugimoto R, Kusunoki T, Yokoyama K, Taniguchi M (2021) Nutrient fluxes from rivers, groundwater, and the ocean into the coastal embayment along the Sanriku ria coast, Japan. Limnol Oceanogr 66: 2728–2744
Nixon SW (1988) Physical energy inputs and the comparative ecology of lake and marine ecosystems. Limnol Oceanogr 33:1005–1025
Ohara K, Yugami Y, Kawahata T, Fujibayashi M, Nishimura O, Sakamaki T (2018) Evaluation of limiting factors of primary production of inner bay using fatty acid composition analysis. J Jpn Soc Civil Eng Ser G (Environ Res) 74:53–61 (in Japanese with English abstract)
Paerl HW, Dennis RL, Whitall DR (2002) Atmospheric deposition of nitrogen: implications for nutrient over-enrichment of coastal waters. Estuaries 25:677–693
Parnell A (2016) Simmr: a stable isotope mixing model. https://cran.r-project.org/package=simmr
R Core Team (2020) R: a language and environment for statistical computing. R Foundation for Statistical Computing, Vienna. https://www.r-project.org/
Redfield AC, Ketchum BH, Richards FA (1963) The influence of organisms on the composition of sea-water. In: Hill MN (ed) The sea, Vol 2. Wiley & Sons, New York, NY, p 26–77
Ruttenberg KC, Dyhrman ST (2012) Dissolved organic phosphorus production during simulated phytoplankton blooms in a coastal upwelling system. Front Microbiol 3:274
Salonen K (1981) Rapid and precise determination of total inorganic carbon and some gases in aqueous solutions. Water Res 15:403–406
Santos IR, Burnett WC, Chanton J, Mwashote B, Suryaputra IG, Dittmar T (2008) Nutrient biogeochemistry in a

Gulf of Mexico subterranean estuary and groundwater-derived fluxes to the coastal ocean. Limnol Oceanogr 53: 705–718

Santos IR, Chen X, Lecher AL, Sawyer AH and others (2021) Submarine groundwater discharge impacts on coastal nutrient biogeochemistry. Nat Rev Earth Environ 2: 307–323

Sarthou G, Timmermans KR, Blain S, Tréguer P (2005) Growth physiology and fate of diatoms in the ocean: a review. J Sea Res 53:25–42

Shiozaki T, Tada Y, Fukuda H, Furuya K, Nagata T (2020) Primary production and nitrogen assimilation rates from bay to offshore waters in the Oyashio-Kuroshio-Tsugaru Warm Current interfrontal region of the northwestern North Pacific Ocean. Deep Sea Res I 164:103304

Slomp CP, Van Cappellen P (2004) Nutrient inputs to the coastal ocean through submarine groundwater discharge: controls and potential impact. J Hydrol (Amst) 295:64–86

Steele JH (1962) Environmental control of photosynthesis in the sea. Limnol Oceanogr 7:137–150

Strickland JDH, Parsons TR (1972) A practical handbook of seawater analysis. Fish Res Board Can Bull 167

Sugimoto R, Kasai A, Miyajima T, Fujita K (2010) Modeling phytoplankton production in Ise Bay, Japan: use of nitrogen isotopes to identify dissolved inorganic nitrogen sources. Estuar Coast Shelf Sci 86:450–466

Sugimoto R, Kitagawa K, Nishi S, Honda H and others (2017) Phytoplankton primary productivity around submarine groundwater discharge in nearshore coasts. Mar Ecol Prog Ser 563:25–33

Suzuki R, Ishimaru T (1990) An improved method for the determination of phytoplankton chlorophyll using N,N-dimethylformamide. J Oceanogr Soc Jpn 46:190–194

Tamborski JJ, Cochran JK, Bokuniewicz HJ (2017) Submarine groundwater discharge driven nitrogen fluxes to Long Island Sound, NY: terrestrial vs. marine sources. Geochim Cosmochim Acta 218:40–57

Tamminen T, Andersen T (2007) Seasonal phytoplankton nutrient limitation patterns as revealed by bioassays over Baltic Sea gradients of salinity and eutrophication. Mar Ecol Prog Ser 340:121–138

Tanaka K, Komatsu K, Itoh S, Yanagimoto D and others (2017) Baroclinic circulation and its high frequency variability in Otsuchi Bay on the Sanriku ria coast, Japan. J Oceanogr 73:25–38

Taniguchi M, Burnett WC, Cable JE, Turner JV (2002) Investigation of submarine groundwater discharge. Hydrol Processes 16:2115–2129

Taniguchi M, Dulai H, Burnett KM, Santos IR and others (2019) Submarine groundwater discharge: updates on its measurement techniques, geophysical drivers, magnitudes, and effects. Front Environ Sci Eng China 7:141

Trommer G, Leynaert A, Klein C, Naegelen A, Beker B (2013) Phytoplankton phosphorus limitation in a North Atlantic coastal ecosystem not predicted by nutrient load. J Plankton Res 35:1207–1219

Turner RE, Rabalais NN (2013) Nitrogen and phosphorus phytoplankton growth limitation in the northern Gulf of Mexico. Aquat Microb Ecol 68:159–169

Unrein F, Massana R, Alonso-Sáez L, Gasol JM (2007) Significant year-round effect of small mixotrophic flagellates on bacterioplankton in an oligotrophic coastal system. Limnol Oceanogr 52:456–469

Watanabe K, Kasai A, Fukuzaki K, Ueno M, Yamashita Y (2017) Estuarine circulation-driven entrainment of oceanic nutrients fuels coastal phytoplankton in an open coastal system in Japan. Estuar Coast Shelf Sci 184:126–137

Welschmeyer NA (1994) Fluorometric analysis of chlorophyll *a* in the presence of chlorophyll *b* and pheopigments. Limnol Oceanogr 39:1985–1992

Yanagi T, Onitsuka G (1999) Numerical model on the lower trophic level ecosystem in Hakata Bay. Umi-no-Kenkyu 8:245–251 (in Japanese with English abstract)

Editorial responsibility: Antonio Bode, A Coruña, Spain
Reviewed by: X. Alvarez-Salgado and 2 anonymous referees

Submitted: October 9, 2022
Accepted: April 25, 2023
Proofs received from author(s): May 29, 2023